

Design Criteria for Transparent Single-Wall Carbon Nanotube Thin-Film Transistors

Husnu Emrah Unalan, Giovanni Fanchini,* Alokik Kanwal, Aurelien Du Pasquier, and Manish Chhowalla*

Materials Science and Engineering, Rutgers University, 607 Taylor Road, Piscataway, New Jersey 08854

Received December 6, 2005; Revised Manuscript Received January 18, 2006

ABSTRACT

A study based on two-dimensional percolation theory yielding quantitative parameters for optimum connectivity of transparent single-wall carbon nanotube (SWNT) thin films is reported. Optimum SWNT concentration in the filtrated solution was found to be 0.1 mg/L with a volume of 30 mL. Such parameters lead to SWNT fractions in the films of approximately $\Phi = 1.8 \times 10^{-3}$, much below the metallic percolation threshold, which is found to be $\sim \Phi_c = 5.5 \times 10^{-3}$. Therefore, the performance of transparent carbon nanotube thin-film transistors is limited by the metallic SWNTs, even below their percolation threshold. We show how this effect is related to hopping or tunneling between neighboring metallic tubes.

Single-wall carbon nanotubes (SWNTs) have been found to exhibit remarkable electronic properties.¹ Although promising results have been obtained for transistors from individual SWNTs,² several inherent properties make it challenging to fabricate devices. Transparent and conducting SWNT networks provide a less lithographically intensive alternative.^{3,4} SWNT thin films represent a new and exciting class of materials in which the SWNTs collectively behave as a random web with high transparency, typical of oxides and insulators, and high conductivity.^{5–7} These properties of SWNT thin films make them suitable replacements for indium tin oxide (ITO). Indeed, recently we have shown that it is possible to replace the ITO electrode in an organic photovoltaic device with transparent and conducting SWNT thin-film electrodes with efficiencies exceeding those of reference devices.⁵ In addition, the room-temperature deposition of SWNT thin films on any substrate has the potential for realization of cheap, flexible, and transparent electronics.

Previously, characterization of SWNT networks has been carried out mainly using models developed for individual nanotubes, bundles, or vertically aligned nanotubes.^{6,7} Recently, Hu et al.⁸ reported the role of the percolation threshold in determining the electrical properties of SWNT thin films. Specifically, their measurements showed that transparent SWNT thin films with tube densities as small as 1.2–1.4 conducting sticks per square micrometer at lengths of $\sim 2 \mu\text{m}$ can be electrically percolating.⁸ Such a small percolation

threshold for SWNTs, in contrast to spheres or disks,⁹ allows the feasibility of very transparent but still metallic SWNT thin films.

In this report, we extend the work of Hu et al.⁸ for insight into the properties of SWNT thin films below the metallic percolation threshold. Our work reveals that the thin films below the percolation threshold are of crucial importance in electronic applications. Indeed, we show that the fabrication of working thin-film transistors can be achieved only much below the percolation threshold. More generally, we have investigated the variation of the thin-film properties as a function of SWNT concentration in the filtrated solution and filtrated volume.

SWNTs synthesized by the high-pressure catalytic decomposition of carbon monoxide method (HiPCO) were purchased from Carbon Nanotechnologies Inc. (batch R0496). As-grown product was then purified thoroughly by low-temperature oxidative annealing and acid treatment as reported by Zhou et al.¹⁰ The process was repeated several times to reduce the concentration of amorphous carbon and metal catalyst particles. Purified SWNTs were sonicated for 2 h in 1 wt % of sodium dodecyl sulfate (SDS) solution. Three different solution concentrations were investigated, namely, $x_{\text{sol}} = 0.2, 1, \text{ and } 2 \text{ mg/L}$ at varying filtrated volumes. Five concentrations ($x_{\text{sol}} = 0.05, 0.1, 0.2, 1, \text{ and } 2 \text{ mg/L}$) were studied at constant filtrated volume, $V_{\text{sol}} = 30 \text{ mL}$.

The SWNT thin films were prepared and transferred onto the substrates according to the procedure developed by Wu et al.⁴ Specifically, water suspensions at different concentra-

* Corresponding authors. E-mail: fanchini@rci.rutgers.edu; manish1@rci.rutgers.edu.

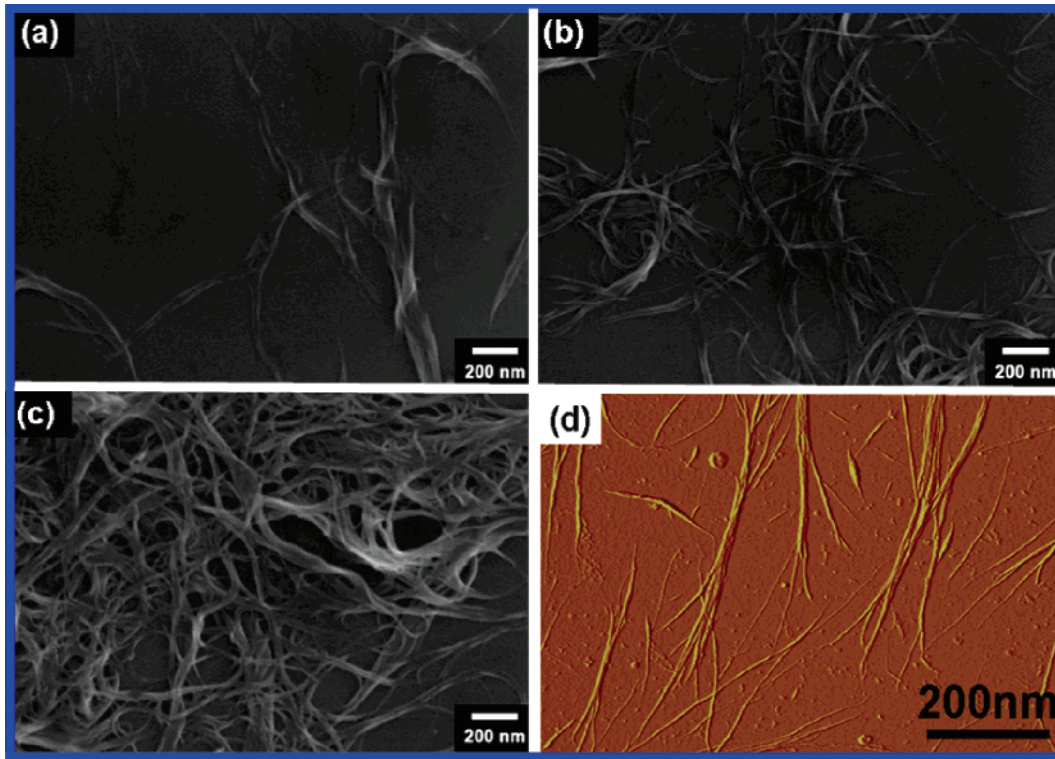


Figure 1. SEM images of SWNT films deposited from 40 mL SWNT solutions of (a) 0.2 mg/L, (b) 1 mg/L, and (c) 2 mg/L concentrations. (d) AFM image of the 1 mg/L SWNT thin films showing a mixture of bundled and individual SWNTs.

tion of SWNTs were filtered on a MCE membrane, which is then attached to the substrate and etched in order to obtain the requisite thin film. The volume of SWNTs in the thin film (V_{NT}) can then be determined by the volume of nanotubes present in the filtrated solution. Bottom-gate transistor devices were prepared by transferring the films on p-type doped silicon substrates coated by a SiO_2 film ($d_{\text{Ox}} = 100$ nm) acting as an insulating layer. Gold source and drain contacts (channel length $20 \mu\text{m}$ and channel width 0.100 mm, total channel area $A_{\text{ch}} = 2 \times 10^{-5} \text{ cm}^2$) were thermally evaporated on the SiO_2 layers using a shadow mask. Transmission measurements were taken using a CHEM 2000 Ocean Optics CCD array fiber optics spectrometer. Films for such measurements were attached on optical-grade fused silica substrates. A standard two-probe technique was used to measure the sheet surface resistivity. The transistor characterization was carried out at room temperature using a computer-controlled HP 4140B picoammeter.

Scanning electron microscope (SEM) and atomic force microscopy (AFM) images of SWNT thin films deposited using different concentrations of SWNTs in a 40 mL filtrate solution are shown in Figure 1. The change in surface coverage can be readily observed. Although nanotubes form a continuous web over the substrate for the 2 mg/L samples (Figure 1c), wide uncovered regions on the substrate can be observed for the 1 mg/L samples as shown in Figure 1b. In Figure 1a, SEM images show the SWNT bundles to be isolated from each other. An AFM image of the 1 mg/L film clearly reveals the presence of both individual and bundled SWNTs. Bundling of the SWNTs can be attributed to insufficient dispersion of our suspension or, more likely, to rebundling during the filtration process.

The normal-incidence transmittance of our SWNT thin films in the 2–5 eV photon energy range is shown in Figure 2. Panels a–c refer to 0.2, 1, and 2 mg/L solution concentrations, respectively. Optical and transport properties correlate very well in our SWNT films, where a clear correlation between the normal-incidence transmittance at 550 nm and the sheet resistance is observed, as shown in Figure 2d.

The conductivity of the SWNT thin films is attributed to the formation of a continuous network that allows efficient current flow primarily through interconnected metallic SWNTs. Such a phenomenon can be described by the percolation theory. As discussed by Hu et al.,⁸ in a series of thin films close to percolation and prepared from a given solution concentration, x_{sol} , the sheet conductance varies as

$$S = C_{\text{met}}(V_{\text{sol}} - V_C)^n \quad (1)$$

where V_{sol} is the solution volume and C_{met} depends on the conductance of the single metallic SWNT. Equation 1 is not universal because both V_C , the critical volume for percolation, and the pre-factor, C_{met} , depend on the concentration, x_{sol} , of the starting solution. Hence, eq 1 must be generalized in order to apply it to varying x_{sol} . In the framework of the theory of percolation, a universal relationship connects¹¹ the metallic conductivity (σ) to the conductivity of the single stick (σ_{met}) and the relative volume fraction $\Phi = V_{\text{NT}}/V$ occupied by the sticks

$$\sigma = \sigma_{\text{met}}(\Phi - \Phi_C)^n \quad (2)$$

In the case of eq 2, and under the assumption of fully random

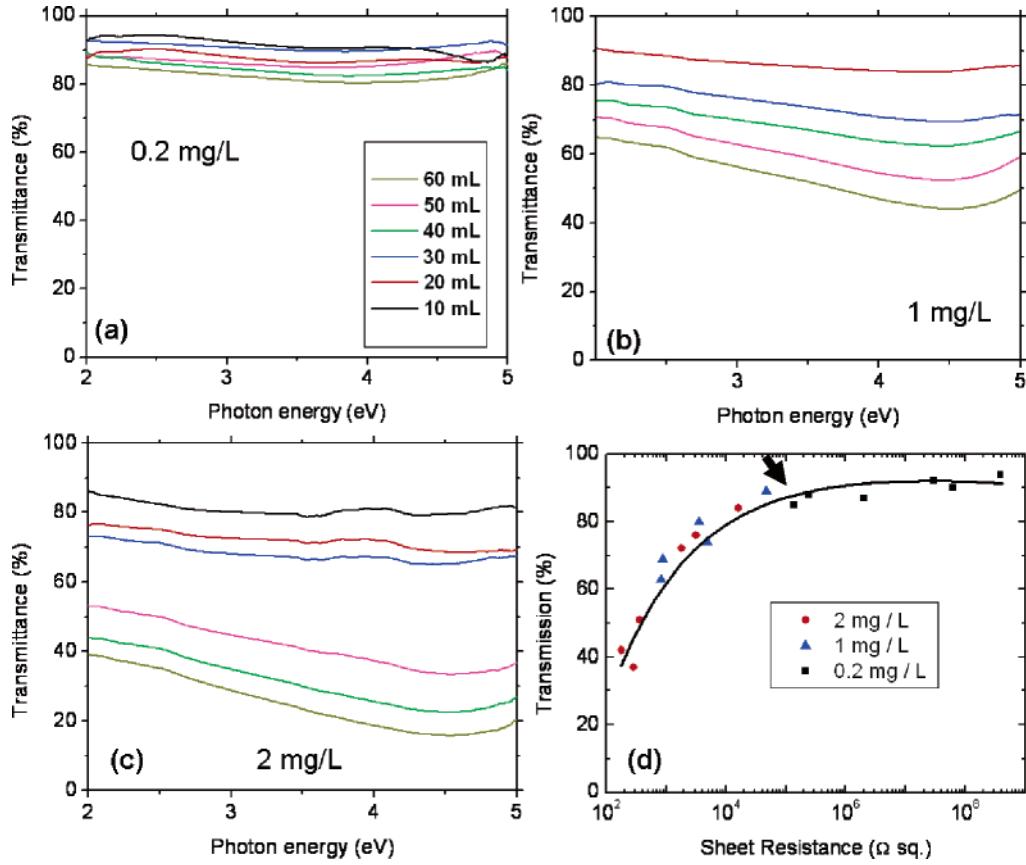


Figure 2. Transmittance of films at three SWNT concentrations [0.2 mg/L (a), 1 mg/L (b), and 2 mg/L (c)] and six different filtrate volumes. (d) Correlation between film transparency (represented by the transmittance at 550 nm) and sheet resistance. The continuous line is a visual aid. The arrow indicates the approximate position of the percolation threshold of the metallic tubes.

networks, the percolation threshold (Φ_C) is independent of Φ , x_{sol} , and V_{sol} and related only to the SWNT length, diameter, and disorder degree.⁹ Φ_C can be expressed as the ratio of the SWNT volume and the “excluded volume”, V_{EX} . The specific excluded volume of the single tube is larger than the tube volume by an amount accounting for the voids remaining between the touching tubes as a consequence of their topology and the topological disorder in the network.⁹ In all of our cases, the networks still contain a relevant fraction of voids, which are necessary for efficient solar cell performance as reported in ref 5. Hence, although some regions are thicker because of the presence of bundles, the SWNT thin films can be on average considered to be formed by no more than one single layer of tubes, especially when approaching the percolation threshold. In such a case, the study of percolation can be restricted to two dimensions because the average film thickness can be estimated to be $d_0 \approx L(\sin \theta)$, depending mainly on the tube length ($L \approx 1 \mu\text{m}$) and their random orientation, θ . The occupied fraction of the SWNT thin films can be estimated to be

$$\Phi = \frac{V_{\text{NT}}}{V_{\text{TOT}}} = \frac{V_{\text{sol}} \frac{x_{\text{sol}}}{\rho_{\text{NT}}}}{A_0 d_0} \approx 6 \times 10^{-4} \cdot V_{\text{sol}} (\text{mL}) \cdot x_{\text{sol}} (\text{mg/L}) \quad (3)$$

where $A_0 = 5 \text{ cm}^2$ is the area of the film, coinciding with the area of the MCE filtering membrane, and a nominal tube

density $\rho_{\text{NT}} = 1.3 \text{ g cm}^{-3}$, which is the average nominal density of tubes at 1–2 nm diameter at different chiralities, is assumed.¹

Figure 3a shows the sheet conductivity of our SWNT thin films spanning almost 7 orders of magnitude because of the changes in the network connectivity. The continuous line in Figure 3a, fitted using eqs 2 and 3, clearly demonstrates a good agreement between the 2D percolation theory and our experimental data. In contrast, in the framework of a 3D model of percolation, d_0 in eq 3 would turn out to be the thickness of the bundles, which we determined, using SEM images on tilted samples, to linearly depend on both V_{sol} and x_{sol} as $d (\text{nm}) \approx 5 \cdot x_{\text{sol}} (\text{mg/L}) \cdot V_{\text{sol}} (\text{mL})$. Assuming most of the SWNTs to be clustered in bundles as required for a 3D percolation model, all of our films would turn out to have the same value of Φ , in strong contradiction with the SEM images. Furthermore, the large variation in conductivities would remain unexplained.

According to the fit in Figure 3a, the metallic percolation threshold is found to be $\Phi_C \approx 5.5 \times 10^{-3}$ and the exponent is $n = 1.65$. These values are in agreement with the 2D percolation theory because there are many reasons for n to be higher than the 2D universal value ($n_0 = 1.33$),¹² which we will address in future work. The conductivity values below the percolation threshold regime (i.e., low Φ) are shown in Figure 3b. In this nonpercolating regime, a mean square fit shows that the data clearly follow an exponential

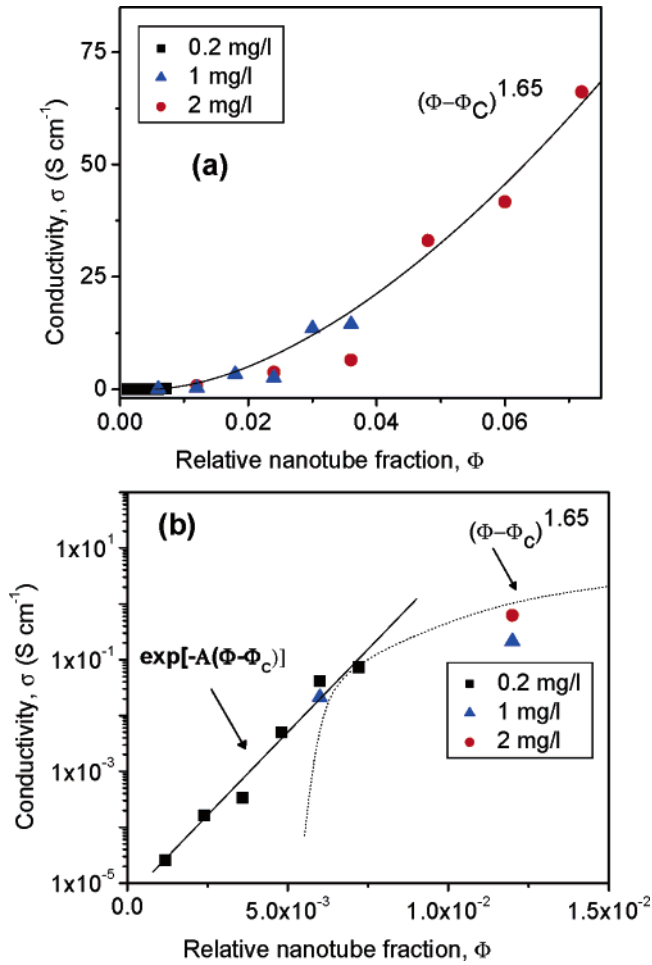


Figure 3. Sheet conductivity versus relative SWNT concentration of our thin films. The line in panel (a) corresponds to a fitting in terms of eq 1. Panel (b) is a semilog magnification of panel (a) at low Φ , showing the trend for the residual conductance below metallic percolation.

law instead of eq 2. Because in a 2D system of tubes $\Phi_C - \Phi$ is related to the intertube distance, Δr , a conduction mechanism based on exponential decay with Δr is likely.

We have tested a wide variation of SWNT concentrations and filtration volumes in order to define an optimum regime for transistor fabrication using SWNT thin films. Because only $2/3$ of the SWNTs are semiconducting in the as-synthesized product, the presence of metallic SWNTs leads to major limitations in the transistor performance, especially the on/off ratios.¹³ Indeed, the metallic SWNTs contribute to the conductivity of the channel even in the off state of a transistor. This has led to the fabrication of SWNT thin-film transistors just below the percolation threshold of metallic tubes, assuming it to be the optimal concentration.¹³ In contrast, we demonstrate through a careful investigation that this condition is not sufficient because even below the metallic percolation threshold the transport properties may still be dominated by the metallic SWNTs.

SWNT thin films prepared from the most concentrated solutions ($x_{\text{sol}} = 1$ and 2 mg/L) always exhibit high carrier density because of high surface coverage, see Figure 1b and c. Even when close to (or below) the metallic percolation threshold, their behavior is dominated by the metallic

SWNTs. Indeed, transistors fabricated from these samples do not exhibit a trans-conductance effect, indicating that these SWNT thin films near the metallic percolation threshold are metallic in their behavior. In the following discussion, we will focus on SWNT thin films produced at concentrations of 0.2 mg/L or less and explore them as semiconducting channels for field-effect transistors.

The output characteristics of SWNT thin-film transistors from three different concentrations ([30 mL, 0.2 mg/L], [30 mL, 0.1 mg/L] and [30 mL, 0.05 mg/L]) are shown in Figure 4a–c, respectively. As shown in Figure 3, the samples we prepared from the 0.2 g/mL solution are always below the metallic percolation threshold. Nevertheless, as exemplified at 30 mL filtrated volume, the performance of our devices is still rather insensitive to channel modulation from the gate (Figure 4a), indicating very little dominance of the hole concentration over the electron concentration as would be expected in a p-type semiconductor. In addition, no clear on/off ratio can be observed from a gate scan of the device (Figure 4d). These results can be understood if we consider that metallic SWNTs of micrometric length have a typical conductance (S_{met}) of $\sim 70 \mu\text{S}$, whereas the conductance of the semiconducting ones is found to be much lower, (S_{sem}) $\sim 1.5 \mu\text{S}$.¹⁴ This would suggest that tunneling (or hopping) between the metallic tubes cannot be neglected. Actually, when the distance Δr between the metallic tubes is low enough to overwhelm the conductivity of the semiconducting ones (as shown schematically in Figure 4e, plot I), the SWNT thin films still exhibit metallic behavior. Tunneling is an exponential effect that dampens with the distance as $\sim \exp(-\alpha \cdot \Delta r)$ ¹⁵ and because in the framework of a 2D percolation model $\Delta r \approx (\Phi_C - \Phi)$, it is an additional argument toward a 2D nature of our material, along with the data in Figure 3b. Hence, a thin-film transistor would have to fulfill the following conditions in order to operate:

$$\sigma_1 \exp[-A(\Phi_C - \Phi)] \ll \sigma_{\text{sem}}(\Phi - \Phi_N)^n \quad (4a)$$

$$\Phi > \Phi_N \quad (4b)$$

where σ_1 is the residual film conductivity at the percolation conditions of metallic tubes and A is related to α , which is the typical out-of-tube decay length of the electronic wave function, determining the tunneling probability. From Figure 3b, we derive σ_1 to be $\sim 100 \text{ S}/\mu\text{m}$ and $A = 7.3 \times 10^{-4}$. Therefore, the exponential factor on the right side of eq 4a must dampen approximately by a factor 100 in order for the semiconducting SWNTs to contribute to the transport properties sufficiently. It should be noted that eq 4 refers to a percolating network in which the metallic SWNTs are not percolating. In such a case, the network conductivity is determined mainly by the semiconducting SWNTs, so the σ_{sem} prefactor in eq 4 is actually close to the conductance of the semiconducting SWNTs. In an ideal fully dispersed SWNT thin film, the percolation threshold of the network would be $\Phi_N = 1/3 \Phi_C$ because $1/3$ of the SWNTs are metallic.

Because none of the samples deposited at the 0.2 mg/L concentration were able to fulfill eq 4a, we explored the

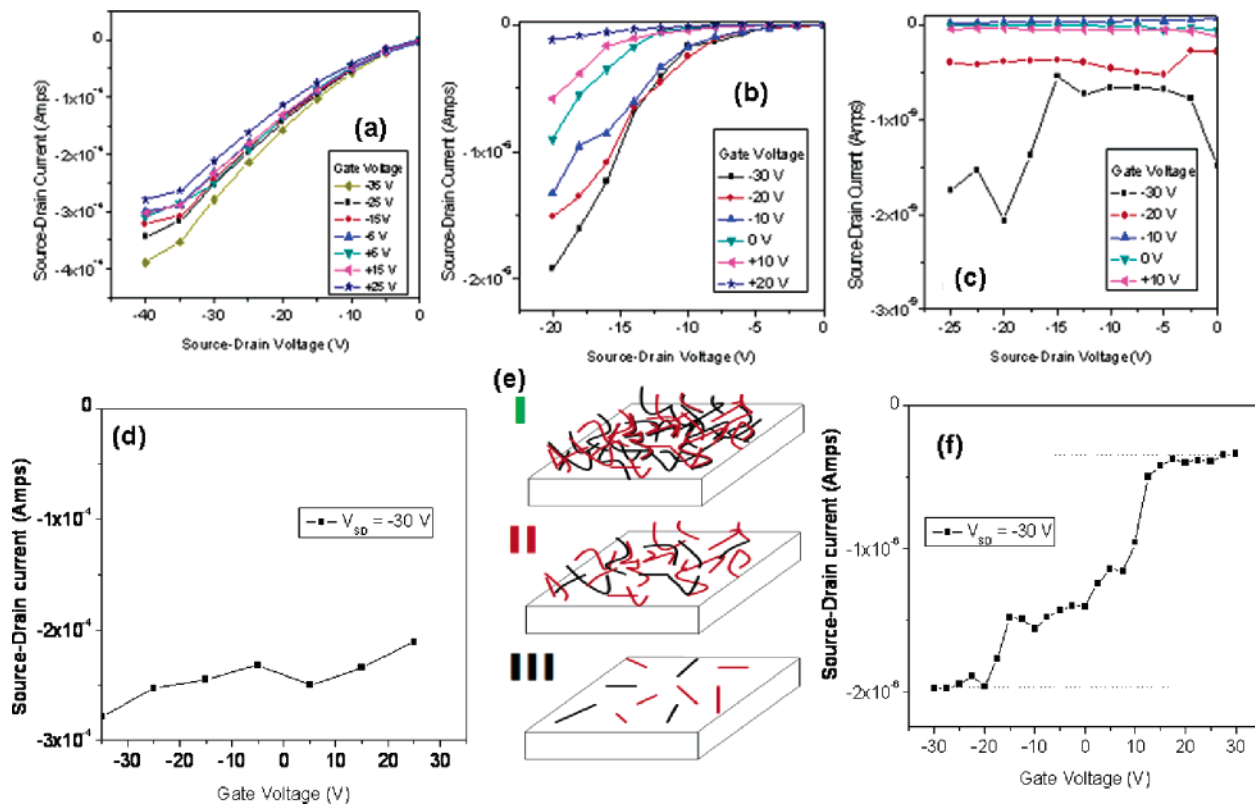


Figure 4. Source–drain scans of (a) device below the percolation threshold of metallic tubes but still dominated by metallic behavior according to eq 4a (30 mL, 0.2 mg/L), (b) transistor in the correct working range (30 mL, 0.1 mg/L), (c) device very much below the network percolation threshold (30 mL, 0.05 mg/L) according to eq 4b. (d) Gate scan (i.e., drain current versus gate voltage) measured at a drain voltage of -30 V for the device in a. (e) Schematic showing (I) a percolating network close to the percolation of metallic tubes, (II) a percolating network far from the percolation of metallic tubes (i.e., the condition obeying to eq 2 and leading to working transistors), and (III) nonpercolating sticks leading to poor transport performance. Metallic tubes are drawn in black, and semiconducting tubes are drawn in red. (f) Gate scan for the working transistor in b.

behavior of thin films prepared by reducing the SWNT concentration in the solution to 0.1 mg/L while keeping the amount of filtrated solution constant at 30 mL ($\Phi = 1.8 \times 10^{-4}$), close to the requirements of eq 4a. Indeed, the reduction of SWNT concentration much below the percolation threshold led to the less dense films with a more remarkable transistor effect, as shown in Figure 4b. Using Figure 4f, the slope of the source–drain current as a function of the gate voltage was measured in the linear region. The field-effect mobility was estimated to be $0.03 \text{ cm}^2/\text{Vs}$. The normalized device transconductance ($\equiv g_m/W$) for a $100 \mu\text{m}$ channel width was found to be $1.2 \times 10^{-6} \text{ S cm}^{-1}$, which is obtained from the saturation region. Although these values are lower than those reported in the literature,^{3,8,13,14} our aim here is not to fabricate state-of-the-art transistors. Instead, our objective is to provide insight into the behavior of SWNT thin films above and below the metallic percolation threshold.

Our results indicate that in order to obtain transistors from SWNT thin films it is important to suppress the percolation between metallic SWNTs while preserving percolation between semiconducting SWNTs within the network. Under such conditions (Figure 4e, plot II) the entire network, formed by metallic and semiconducting SWNTs, is still percolating or close to percolation, giving rise to sufficient field effect mobility. Our SEM and AFM images in Figure 1 reveal the presence of bundles along with fully dispersed SWNTs.

Although our suspensions are fully dispersed, some bundling does occur during the filtration process. However, we argue that eq 4 in our model is valid even in a nonideally dispersed system. In a case involving bundles, $\Phi_N > \frac{1}{3}\Phi_C$ reduces the window of Φ values given by eq 4, in which transistor effect may be observed. In the most pessimistic case of a fully nondispersed SWNT system, the percolation threshold of the entire network coincides with the metallic threshold, $\Phi_N \approx \Phi_C$, and no transistor effect can be observed. This is not the case here because transistor effect is clearly observed in our thin films. In our work, an intermediate case where the bundles are somewhat isolated from each other is more appropriate. In such a case, the conductivity, far from percolation, of the system is mainly from individual SWNTs. Because statistically $\frac{1}{3}$ are metallic and $\frac{2}{3}$ semiconducting, the presence of a fraction of SWNTs leads to lower Φ_C and Φ_N without affecting the validity of the 2D percolation model. Therefore, determining the lower concentration limit of a working transistor allows us to estimate the structural organization of our SWNT thin films. At further dilution of our solutions ($x_{\text{sol}} = 0.05 \text{ mg/L}$ and below, at $V_{\text{sol}} = 30 \text{ mL}$, $\Phi = 9 \times 10^{-4}$), we have nonconnected networks. The conductance falls below 1 nA, and the transistor performance is limited by the breakdown of our SiO_2 insulator, as indicated in Figure 4c. Therefore, in our case the network percolation threshold, Φ_N , can be set between 9×10^{-4} and

1.8×10^{-3} . At these low concentrations, the SEM images show the SWNT bundles to be isolated. Because the metallic percolation threshold was found to be at $\Phi_C \approx 5.5 \times 10^{-3}$, we note that the presence of bundles does not affect the ratio between Φ_C and Φ_N , which remains close to $1/3$. Rather, the presence of bundles limits the on/off ratio of our devices in the working range given by eq 4.

In conclusion, we have discussed the optoelectronic properties of SWNT thin films and the influence of percolation on thin-film-transistor characteristics. Quantitative application of the 2D theory of percolation allowed us to study, for the first time, the subpercolation tunneling behavior of SWNT networks. The performance of transparent SWNT thin-film transistors has been shown to be limited by metallic SWNTs, even much below their percolation threshold. Transistor performance can be improved by depositing SWNT thin films from solutions enriched with semiconducting SWNTs.¹⁶ This sets the percolation of the metallic SWNT to higher values, allowing the exploitation of semiconducting networks at higher densities.

Acknowledgment. We acknowledge financial support from the U.S.–Israel Binational Fund and the Rutgers University Academic Excellence Fund.

References

- (1) *Carbon Nanotubes: Synthesis, Structure, Properties, and Applications*; Dresselhaus, M. S.; Dresselhaus, G.; Avouris, P., Eds.; Springer-Verlag: New York, 2001.

- (2) Bachtold, A.; Hadley, P.; Nakanishi, T.; Dekker, C. *Science* **2001**, *294*, 1317.
- (3) Artukovic, E.; Kaempgen, M.; Hecht, D. S.; Roth, S.; Gruner, G. *Nano Lett.* **2005**, *5*, 757.
- (4) Wu, Z.; Chen, Z.; Du, X.; Logan, J. M.; Sippel, J.; Nikolou, M.; Kamaras, K.; Reynolds, J. R.; Tanner, D. B.; Hebard, A. F.; Rinzler, A. G. *Science* **2004**, *305*, 1273.
- (5) Du Pasquier, A.; Unalan, H. E.; Kanwal, A.; Miller, S.; Chhowalla, M. *Appl. Phys. Lett.* **2005**, *87*, 203511.
- (6) De Heer, W.; Bacsá, W. S.; Chatelain, A.; Gerfin, T.; Humphrey-Baker, R.; Forro, L. *Science* **1995**, *268*, 845.
- (7) Saran, N.; Parikh, K.; Suh, D. S.; Munoz, E.; Kolla, H.; Manohar, S. K. *J. Am. Chem. Soc.* **2004**, *126*, 4462.
- (8) Hu, L.; Hecht, D. S.; Gruner, G. *Nano Lett.* **2004**, *4*, 2513.
- (9) Balberg, I.; Anderson, C.; Alexander, S.; Wagner, N. *Phys. Rev. B* **1984**, *30*, 3933.
- (10) Zhou, W.; Ooi, Y. H.; Russo, R.; Papanek, P.; Luzzi, D. E.; Fischer, J. E.; Bronikowski, M. J.; Willis, P. A.; Smalley, R. E. *Chem. Phys. Lett.* **2001**, *350*, 6.
- (11) Stauffer, D.; Aharony, A. *Introduction to Percolation Theory*; Taylor & Francis: London, 1992.
- (12) Sahimi, M. *Applications of Percolation Theory*; Taylor & Francis: London, 1994.
- (13) Snow, E. S.; Novak, J. P.; Campbell, P. M.; Park, D. *Appl. Phys. Lett.* **2003**, *82*, 2145.
- (14) Martel, R.; Schmidt, T.; Shea, H. R.; Avouris, P. *Appl. Phys. Lett.* **1998**, *73*, 2447.
- (15) Mott, N. F.; Davis, E. A. *Electronic Processes in Noncrystalline Materials*; Clarendon: Oxford, 1979; p 33.
- (16) Johnston, D.; Islam, M. F.; Yodh, A. G.; Johnson, A. T. *Nat. Mater.* **2005**, *4*, 589.

NL052406L